On the Noise Behavior of a SAW Convolver Used as a Matched Filter

Gerald Ostermayer, *Associate Member, IEEE*

***Abstract*—The noise behavior of a surface acoustic wave convolver used as an analog matched filter is investigated in this paper. In contrast to the existing literature, we do not neglect the influence of noise processes with squared amplitudes. It is shown that these quadratic noise contributions have a significant influence on the output signal-to-noise ratio (SNR) of the convolver for values of input SNR lower than 10 dB. The calculation is done for on-off keying coded signals but the results are also valid for other modulation schemes, e.g., phase shift keying.**

***Index Terms*—Convolver, matched filter, noise, SAW, spread spectrum.**

I. Introduction

In THE LAST years, several interesting applications of surface acoustic wave (SAW) convolvers were published [1]–[5]. This device was used in spread-spectrum communication systems, measurement systems, and sensing systems. Whenever a real-time correlation of fast varying signals with high time-bandwidth product is necessary a SAW convolver can advantageously be used. This is due to its high real-time calculation capability for a specific operation, i.e., for convolution or correlation, respectively. For signal detection in communication systems, as well as for accuracy estimation in measurement and sensing systems, the influence of noise at the convolver inputs to the output signal is extremely interesting.

In Section II, a short description of a SAW convolver is given. Section III describes how noise at the convolver inputs affect the signal at the output. Finally, short conclusions are given in Section IV.

II. SAW Convolver

A SAW convolver is an electroacoustic device with three electrical ports: two input and one output port [6]. The electrical signal $c(t)$ at the convolver output is strongly related to the continuous-time convolution of the two electrical input signals $r(t)$ and $s(t)$. Fig. 1 shows a SAW convolver. At each end of the piezoelectric substrate, there is an interdigital transducer (IDT) [7]. The IDT element consists of an electrical and acoustic port and converts the electrical input signals $r(t)$ and $s(t)$ into the propagating acoustic waves $r_a(t,x) = r(t-(L/2+x)/v_s)$ and $s_a(t,x) = s(t-(L/2-x)/v_s)$, with v_s being the sound velocity. Each IDT is followed by a beam compressor, which compresses the beam width to a couple of wavelengths. Between the beam compressors, there is a narrow (a few wavelengths) metallic electrode of length L_i. Below this waveguide, the signals $r_a(t,x)$ and $s_a(t,x)$ propagate in opposite directions. Due to the large-signal amplitudes in this area, a local polarization is generated, which is proportional to $(r_a(t,x)+s_a(t,x))^2$, i.e., the local product $r_a(t,x)\cdot s_a(t,x)$ is generated. The long metallic electrode integrates the surface polarization over L_i. If the electrode is very long compared to the wavelength, the integration of all polarization parts not contributing to the convolution operation results in a constant offset of the output signal. Due to capacitive coupling of the convolver ports, this offset does not affect the output signal. Introducing integration time $T_i = L_i/v_s$ and defining $\tau = x/v_s$, we get for the convolver output signal

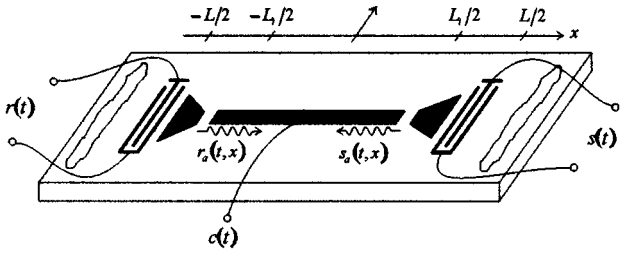

Fig. 1. Principle structure of a SAW convolver.

$$c\left(t+\frac{T_i}{2}+T_d\right) = v_s k \cdot \int_{-(T_i/2)}^{T_i/2} s(t+\tau)\cdot r(t-\tau)\,d\tau \qquad (1)$$

with k as a proportionality factor and $T_d = (L-L_i)/2v_s$ as the delay due to the distance between IDT and waveguide. It is seen that the output signal $c(t)$ is a time-compressed (with a factor of two) and time-delayed $(T_i/2+T_d)$ version of the convolution of the input signals $r(t)$ and $s(t)$. Due to the time compressing, it is possible to design a convolver in a way that the input and output spectrums do not cover the same frequency range. Thus, input and output signals are not disturbed by crosstalk. With a suitable choice of $r(t)$, an analog real-time matched filter for almost arbitrarily signals $s(t)$ can be built.

III. Noise Behavior

A. General

In this section, we investigate how the convolver output signal is affected by noise at the inputs. In the literature [8], one can find such calculations with much more simplifications, as in this paper. Our focus lies on the use of a convolver as a matched filter. We investigate the dependence of the SNR at the sampling moment of the output signal on the SNRs of the two input signals.

Manuscript received October 25, 2000; revised January 15, 2001.

The author is with PSE MCS RA 2, Siemens AG Österreich, A-1101 Vienna, Austria.

Publisher Item Identifier S 0018-9480(01)02903-9.

Basis for our calculations in the time domain is the general relation between the electrical input signals $r(t)$ and $s(t)$ (corrupted by mutually uncorrelated white Gaussian noise processes $n_r(t)$ and $n_s(t)$, respectively) and the electrical output signal $c(t)$ [6]

$$\begin{aligned} c(t) = & \int_{-(T_i/2)}^{T_i/2} \Big\{ c_L \big[s(t+\tau) + n_s(t+\tau) + r(t-\tau) \\ & + n_r(t-\tau) \big] \Big\} \, d\tau \\ & + \int_{-(T_i/2)}^{T_i/2} \Big\{ c_{\mathrm{NL}} \big[s(t+\tau) + n_s(t+\tau) + r(t-\tau) \\ & + n_r(t-\tau) \big]^2 \Big\} \, d\tau \end{aligned} \tag{2}$$

with c_L as the weighting factor for the linear relationship between the inputs and output, c_{NL} as the weighting factor for the quadratic nonlinear relationship between the inputs and output, $s(t)$ as a convolver input signal (receiving signal), $r(t)$ as the other convolver input signal (reference signal), $c(t)$ as the convolver output signal, T_i as the time duration of the integrating electrode, $n_s(t)$ as a stationary noise process at input s with two-sided power spectral density η_s, and $n_r(t)$ as a stationary noise process at input r with two-sided spectrum density η_r. The convolver itself is considered to be noise free. Rewriting (2) gives

$$\begin{aligned} & c(t) \\ & = \underbrace{c_L \int_{-(T_i/2)}^{T_i/2} s(t+\tau)\, d\tau}_{\text{time independent}} + \underbrace{c_L \int_{-(T_i/2)}^{T_i/2} r(t-\tau)\, d\tau}_{\text{time independent}} \\ & + \underbrace{c_L \int_{-(T_i/2)}^{T_i/2} n_s(t+\tau)\, d\tau}_{\text{neglectible}} + \underbrace{c_L \int_{-(T_i/2)}^{T_i/2} n_r(t-\tau)\, d\tau}_{\text{neglectible}} \\ & + \underbrace{c_{\mathrm{NL}} \int_{-(T_i/2)}^{T_i/2} s^2(t+\tau)\, d\tau}_{\text{time independent}} + \underbrace{c_{\mathrm{NL}} \int_{-(T_i/2)}^{T_i/2} r^2(t-\tau)\, d\tau}_{\text{time independent}} \\ & + \underbrace{c_{\mathrm{NL}} \int_{-(T_i/2)}^{T_i/2} n_s^2(t+\tau)\, d\tau}_{n_s n_s(t)} + \underbrace{c_{\mathrm{NL}} \int_{-(T_i/2)}^{T_i/2} n_r^2(t-\tau)\, d\tau}_{n_r n_r(t)} \\ & + \underbrace{c_{\mathrm{NL}} \cdot 2 \int_{-(T_i/2)}^{T_i/2} s(t+\tau) \cdot r(t-\tau)\, d\tau}_{sr(t)} \\ & + \underbrace{c_{\mathrm{NL}} \cdot 2 \int_{-(T_i/2)}^{T_i/2} s(t+\tau) \cdot n_s(t+\tau)\, d\tau}_{sn_s(t)} \\ & + \underbrace{c_{\mathrm{NL}} \cdot 2 \int_{-(T_i/2)}^{T_i/2} s(t+\tau) \cdot n_r(t-\tau)\, d\tau}_{sn_r(t)} \\ & + \underbrace{c_{\mathrm{NL}} \cdot 2 \int_{-(T_i/2)}^{T_i/2} r(t-\tau) \cdot n_r(t-\tau)\, d\tau}_{rn_r(t)} \end{aligned}$$

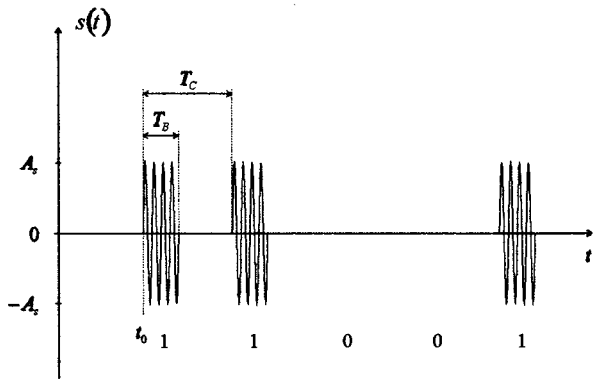

Fig. 2. Example of an OOK coded signal with $\varphi_s = -\pi/2$ and code [1 1 0 0 1].

$$\begin{aligned} & + \underbrace{c_{\mathrm{NL}} \cdot 2 \int_{-(T_i/2)}^{T_i/2} r(t-\tau) \cdot n_s(t+\tau)\, d\tau}_{rn_s(t)} \\ & + \underbrace{c_{\mathrm{NL}} \cdot 2 \int_{-(T_i/2)}^{T_i/2} n_s(t+\tau) \cdot n_r(t-\tau)\, d\tau}_{\text{negectible}} . \end{aligned} \tag{3}$$

Without loss of generality, we concentrate on on–off keying (OOK) coded signals since, at some points, the calculations are simpler than, for example, phase-shift keying (PSK) coded signals. Note that all derived results for the sampling moment are valid for other coding schemes (binary phase-shift keying (BPSK), quaternary phase-shift keying (QPSK), ...) as well. The time duration T_C is the chip duration, T_B is the duration of the RF burst in case a chip is set to "1." We consider the general case for $T_C \neq T_B$, but in practice, T_C and T_B are often the same, i.e., $T_C = T_B$. Signal s can be written as

$$\begin{aligned} s(t) = \; & A_s \sum_{k=1}^{N} \Big\{ \mathrm{code}(k,n) \cdot s_{LP}\big(t - t_0 - (k-1)T_C\big) \\ & \times \cos\Big[\omega_s\big(t - t_0 - (k-1)T_C\big) + \varphi_s\Big] \Big\} \end{aligned} \tag{4}$$

with $s_{LP}(t) = \mathrm{rect}((t - T_B/2)/T_B/2)$ as the burst envelope and $\mathrm{rect}(t) = 1$ for $|t| < 1$, $\mathrm{rect}(t) = 0$ otherwise, as the normalized rectangle function. A_s denotes the amplitude, and $\mathrm{code}(k,n)$ denotes the signal code of length N with n chips set to "1." Fig. 2 shows an example. Analogously, the reference signal can be written as

$$\begin{aligned} r(t) = \; & A_r \sum_{k=1}^{N} \Big\{ \mathrm{code}(k,n) \cdot r_{LP}\big(t - t_0 - (k-1)T_C\big) \\ & \times \cos\Big[\omega_r\big(t - t_0 - (k-1)T_C\big) + \varphi_r\Big] \Big\} \end{aligned} \tag{5}$$

with $r_{LP}(t) = \mathrm{rect}((t - T_B/2)/T_B/2)$. Before we start the evaluation of (3), some assumptions are stated. The maximum code duration has to be shorter than the integrating electrode of the convolver. The sampling point of the output signal equals the moment when the receiving and reference signals completely overlap. The system has to make sure that, at this moment, both signals are completely covered by the integrating electrode. A

suitable choice of t_0 in (4) and (5) guarantees that this prerequisite is fulfilled.

B. Irrelevant Signals

Parts 1, 2, 5, and 6 of (3) are integrals of sinusoidal waves [cf (4) and (5)]. As stated in the above section, we are only interested in the conditions at the sampling moment. At this time, whole signals $r(t)$ and $s(t)$ are covered by the integrating electrode. Therefore, calculating parts 1, 2, 5, and 6 of (3) result in time-independent values. Due to capacitive coupling, such an offset does not appear at the convolver output and, therefore, needs not be considered. Parts 3 and 4 of (3) can be neglected since the noise processes $n_s(t)$ and $n_r(t)$ have zero mean and the integrating time T_i is much longer than the inverse of the convolver input bandwidth. Since $n_s(t)$ and $n_r(t)$ are uncorrelated processes, the last part of (3) can be neglected as well.

C. Relevant Signals

Seven parts of (3) remain, which contribute to the convolver output signal: $sr(t)$, $sn_s(t)$, $sn_r(t)$, $rn_r(t)$, $rn_s(t)$, $n_sn_s(t)$, and $n_rn_r(t)$. The signal $sr(t)$ of (3) is the desired output signal. All other signals are noise processes, which disturb $sr(t)$. It is a special property of a convolver that the noise power partly depends on the input signals $s(t)$ and $r(t)$. In the following, we will calculate the power or variance of all parts of the output signal at the sampling moment to find the relationship between the SNR of the output signal (at sampling moment) and the SNRs of the input signals.

1) Desired Output Signal: At the sampling moment $(t = 0)$, all chips of $s(t)$ and $r(t)$ are exactly time aligned. From (4) and (5), we know that an optimum correlation result is given for $\varphi_r = -\varphi_s$. Fig. 3 shows chips k of the signals $s(t+\tau)$ and $r(t-\tau)$. The arrows indicate the signal propagation direction for increasing time. For the following considerations, we assume $T_C > 2T_B$. This guarantees that each chip overlaps with, at most, one other chip. The value of the correlation maximum is not affected by this assumption. Therefore, the results at $t = 0$ of these investigations are valid for $T_B \le T_C$. With (4) and (5), we get

$$\begin{aligned} sr(t) &= 2c_{\mathrm{NL}} \cdot \int_{-(T_i/2)}^{T_i/2} s(t+\tau) \cdot r(t-\tau)\, d\tau \\ &= 2c_{\mathrm{NL}} A_s A_r \cdot \sum_{k=1}^{N} \int_{-(T_i/2)}^{T_i/2} \\ &\quad \cdot \Big\{ \mathrm{code}^2(k,n) \cdot s_{LP}\big(t+\tau-t_0-(k-1)T_C\big) \\ &\qquad \times r_{LP}\big(t-\tau+t_0+(k-1)T_C\big) \\ &\qquad \cdot \cos\Big[\omega_s\big(t+\tau-t_0-(k-1)T_C\big)+\varphi_s\Big] \\ &\qquad \times \cos\Big[\omega_r\big(t-\tau+t_0+(k-1)T_C\big)+\varphi_r\Big] \Big\}\, d\tau. \end{aligned} \tag{6}$$

The integration limits are taken from Fig. 3. Within these limits, it is guaranteed that $s_{LP} \cdot r_{LP} = 1$. Again, we assume

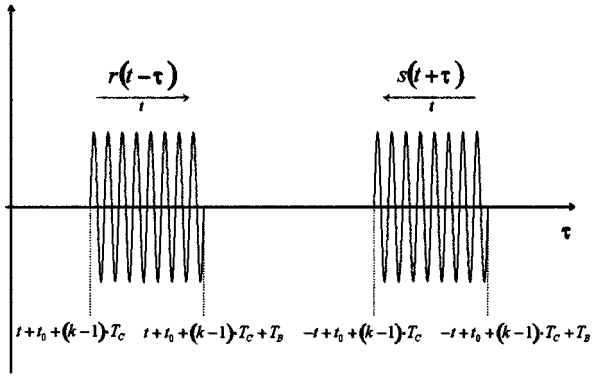

Fig. 3. The kth bits of the signals $s(t+\tau)$ and $r(t-\tau)$.

(without loss of generality) that the code length is n and all chips are set to "1."

Additionally, we agree on $\omega_s = \omega_r = \omega_{\mathrm{in}}$. With these assumptions, we get

$$s_r(t) = \begin{cases} 2c_{\mathrm{NL}} \cdot \dfrac{A_s A_r}{2} \cdot n \cdot 2 \cdot \cos(2\omega_{\mathrm{in}} t + \varphi_s + \varphi_r) \\ \quad \cdot \left(t + \dfrac{T_B}{2}\right) + 2c_{\mathrm{NL}} \cdot \dfrac{A_s A_r}{2} \cdot n \\ \quad \cdot \dfrac{\sin(2\omega_{\mathrm{in}} t + \omega_{\mathrm{in}} T_B) \cdot \cos(\omega_{\mathrm{in}} T_B + \varphi_s + \varphi_r)}{\omega_{\mathrm{in}}}, \\ \qquad -\dfrac{T_B}{2} \le t < 0 \\ 2c_{\mathrm{NL}} \cdot \dfrac{A_s A_r}{2} \cdot n \cdot 2 \cdot \cos(2\omega_{\mathrm{in}} t + \varphi_s + \varphi_r) \\ \quad \cdot \left(-t + \dfrac{T_B}{2}\right) + 2c_{\mathrm{NL}} \cdot \dfrac{A_s A_r}{2} \cdot n \\ \quad \cdot \dfrac{\sin(-2\omega_{\mathrm{in}} t + \omega_{\mathrm{in}} T_B) \cdot \cos(\omega_{\mathrm{in}} T_B + \varphi_s + \varphi_r)}{\omega_{\mathrm{in}}}, \\ \qquad 0 \le t < \dfrac{T_B}{2}. \end{cases} \tag{7}$$

Since relevant frequency values are in the range of several 100 MHz, the parts with ω_{in} in the denominator can be neglected. With $\Lambda(t) = 1 - |t|$ for $|t| < 1$, $\Lambda(t) = 0$, otherwise we get

$$\begin{aligned} sr(t) = \; & 2c_{\mathrm{NL}} \cdot \frac{A_s A_r}{2} \cdot n \cdot T_B \cdot \Lambda\left(\frac{2t}{T_B}\right) \\ & \cdot \cos\left(2\omega_{\mathrm{in}} t + \varphi_s + \varphi_r\right). \end{aligned} \tag{8}$$

The maximum can be calculated to $sr(t = 0, \varphi_r = -\varphi_s) = SR = c_{\mathrm{NL}} \cdot A_s A_r \cdot n \cdot T_B$. The power is given by

$$P_{SR} = 4c_{\mathrm{NL}}^2 \cdot \frac{A_s^2 A_r^2}{4} \cdot (nT_B)^2. \tag{9}$$

2) Quadratic Noise Signals: In contrast to previous literature (e.g., [8]), the quadratic noise signals $n_rn_r(t)$ and $n_sn_s(t)$ [cf (3)] are not neglected in this paper. We will see that these signals have a significant influence on the SNR of the convolver output signal. In the following, we calculate the power P_{nrnr} and the variance σ_{nrnr}^2 of the noise process $n_rn_r(t)$. The noise process is assumed to be stationary, white, and Gaussian with a two-sided spectrum density η_r. The noise power is given by

$$P_{n_rn_r} = \frac{1}{2\pi} \cdot \int_{-\infty}^{\infty} \Phi_{n_rn_r}(\omega)\, d\omega \tag{10}$$

with $\Phi_{nrnr}(\omega) = \mathrm{FT}\{\varphi_{nrnr}(\tau)\}$ and $\varphi_{nrnr}(\tau) = \mathrm{ACF}\{n_r n_r(t)\}$, where FT and ACF denote the Fourier transform and the autocorrelation function, respectively. The noise process $n_r n_r(t)$ can be written as

$$\begin{aligned} n_r n_r(t) &= c_{\mathrm{NL}} \cdot \int_{-(T_i/2)}^{T_i/2} n_r^2(t-\tau)\, d\tau \\ &= \int_{-\infty}^{\infty} c_{\mathrm{NL}} \cdot \mathrm{rect}\left(\frac{2\tau}{T_i}\right) \cdot n_r^2(t-\tau)\, d\tau \\ &= \int_{-\infty}^{\infty} h(\tau) \cdot n_r^2(t-\tau)\, d\tau \\ &= h(t) * n_r^2(t) \end{aligned} \tag{11}$$

with $h(t) = c_{\mathrm{NL}} \cdot (\mathrm{rect}(2t/T_i)$. The relationship between the power spectral densities of a stationary process $n_r^2(t)$ at the input and a stationary process $n_r n_r(t)$ at the output of a linear time invariant (LTI) system is given by

$$\Phi_{n_r n_r}(\omega) = \Phi_{n_r^2}(\omega) \cdot \left|H(j\omega)\right|^2$$

[9]. The relationship between the ACFs of a stationary noise process $n_r(t)$ and the same process with squared amplitudes $n_r^2(t)$ is given by

$$\Phi_{n_r^2}(\omega) \overset{\mathrm{FT}}{\longleftrightarrow} \varphi_{n_r^2}(\tau) = \sigma_{n_r}^4 + 2 \cdot \varphi_{n_r}^2(\tau)$$

where FT denotes the Fourier transform [10]. Consequently, we get for the power spectrum density of $n_r n_r(t)$

$$\begin{aligned} \Phi_{n_r n_r}(\omega) &= \mathrm{FT}\left\{\sigma_{n_r}^4\right\} \cdot \left|H(j\omega)\right|^2 \\ &\quad + 2 \cdot \mathrm{FT}\left\{\varphi_{n_r}^2(\tau)\right\} \cdot \left|H(j\omega)\right|^2 \\ &= 2\pi \cdot \sigma_{n_r}^4 \cdot \left|H(j\omega)\right|^2 \cdot \delta(\omega) \\ &\quad + \frac{1}{\pi} \cdot \left|H(j\omega)\right|^2 \cdot \Phi_{n_r}(\omega) * \Phi_{n_r}(\omega). \end{aligned} \tag{12}$$

At the convolver input, we assume to have an ideal passband filter with center frequency f_0 and bandwidth $2 \cdot f_g$. The noise power spectrum density after that filter can be written as

$$\Phi_{n_r}(\omega) = \eta_r \cdot \left[\mathrm{rect}\left(\frac{\omega-\omega_0}{\omega_g}\right) + \mathrm{rect}\left(\frac{\omega+\omega_0}{\omega_g}\right)\right]. \tag{13}$$

The convolution of this noise power spectrum density gives

$$\begin{aligned} &\Phi_{n_r}(\omega) * \Phi_{n_r}(\omega) \\ &\quad = 2\omega_g \cdot \eta_r^2 \\ &\qquad \times \left[\Lambda\left(\frac{\omega-2\omega_0}{2\omega_g}\right) + \Lambda\left(\frac{\omega+2\omega_0}{2\omega_g}\right) + 2 \cdot \Lambda\left(\frac{\omega}{2\omega_g}\right)\right]. \end{aligned} \tag{14}$$

From (11), we know

$$\left|H(j\omega)\right|^2 = c_{\mathrm{NL}}^2 \cdot \frac{4}{\omega^2} \cdot \sin^2\left(\omega\frac{T_i}{2}\right).$$

Knowing this and using (10), (12), and (14), we yield for the power P_{nrnr} of $n_r n_r(t)$

$$\begin{aligned} P_{n_r n_r} &= 4c_{\mathrm{NL}}^2 \sigma_{n_r}^4 \cdot \int_{-\infty}^{\infty} \frac{\sin^2\left(\omega\frac{T_i}{2}\right)}{\omega^2} \delta(\omega)\, d\omega \\ &\quad + c_{\mathrm{NL}}^2 \frac{4}{\pi^2} \omega_g \eta_r^2 \times \int_{-\infty}^{\infty} \frac{\sin^2\left(\omega\frac{T_i}{2}\right)}{\omega^2} \\ &\quad \cdot \left[\Lambda\left(\frac{\omega-2\omega_0}{2\omega_g}\right) + \Lambda\left(\frac{\omega+2\omega_0}{2\omega_g}\right) + 2\Lambda\left(\frac{\omega}{2\omega_g}\right)\right] d\omega. \end{aligned} \tag{15}$$

The variance σ_{nrnr}^2 equals the power P_{nrnr} minus the contribution at $\omega = 0$. Thus, we get for the variance σ_{nrnr}^2 of $n_r n_r(t)$

$$\begin{aligned} \sigma_{n_r n_r}^2 = \; & c_{\mathrm{NL}}^2 \frac{4}{\pi^2} \omega_g \eta_r^2 \times \int_{-\infty}^{\infty} \frac{\sin^2\left(\omega\frac{T_i}{2}\right)}{\omega^2} \\ & \cdot \left[\Lambda\left(\frac{\omega-2\omega_0}{2\omega_g}\right) + \Lambda\left(\frac{\omega+2\omega_0}{2\omega_g}\right) + 2\Lambda\left(\frac{\omega}{2\omega_g}\right)\right] d\omega. \end{aligned} \tag{16}$$

Considering the relation [11]

$$\begin{aligned} &\mathrm{Ci}(x) = \gamma + \ln(x) + \int_0^x \frac{\cos(t)-1}{t} dt \\ &\left|\arg(x)\right| < \pi, \qquad \text{with } \gamma = 05772156649 \end{aligned} \tag{17}$$

(16) can be rewritten into

$$\begin{aligned} \sigma_{n_r n_r}^2 = \; & c_{\mathrm{NL}}^2 \frac{4}{\pi^2} \eta_r^2 \\ & \cdot \Bigg\{ -\gamma - 1 + \ln\left(\frac{\omega_0}{2\omega_g\sqrt{\omega_0^2 - \omega_g^2}}\right) \\ & + \underbrace{\cos\left(2\omega_0 T_i\right) \cdot \cos\left(2\omega_g T_i\right)}_{-1\,(\text{worst case})} \\ & + \underbrace{2\sin\left[(\omega_0+\omega_g)T_i\right] \cdot \sin\left[(\omega_0-\omega_g)T_i\right]}_{-2\,(\text{worst case})} \\ & - 2\omega_0 T_i \cdot \underbrace{\mathrm{Si}\left(2\omega_0 T_i\right)}_{\approx\pi/2} + 2\omega_g T_i \cdot \underbrace{\mathrm{Si}\left(2\omega_g T_i\right)}_{\approx\pi/2} \\ & + \left(\omega_0+\omega_g\right)T_i \cdot \underbrace{\mathrm{Si}\Big[2\left(\omega_0+\omega_g\right)T_i\Big]}_{\approx\pi/2} \\ & + \left(\omega_0-\omega_g\right)T_i \cdot \underbrace{\mathrm{Si}\Big[2\left(\omega_0-\omega_g\right)T_i\Big]}_{\approx\pi/2} \\ & - \underbrace{\mathrm{Ci}\left(2\omega_0 T_i\right)}_{\approx 0} + \underbrace{\mathrm{Ci}\left(2\omega_0 T_i\right)}_{\approx 0} + \frac{1}{2} \\ & \cdot \underbrace{\mathrm{Ci}\Big[2\left(\omega_0+\omega_g\right)T_i\Big]}_{\approx 0} + \frac{1}{2} \cdot \underbrace{\mathrm{Ci}\Big[2\left(\omega_0-\omega_g\right)T_i\Big]}_{\approx 0} \Bigg\}. \end{aligned} \tag{18}$$

For arguments $x > 100$ $\mathrm{Si}(x)$ and $\mathrm{Ci}(x)$ can be very well approximated by $\pi/2$ and zero. Since the frequency range and integration length of a SAW convolver is in the range of some 100 MHz and some microsecond, respectively, the condition $x > 100$ is fulfilled very well. For instance, the argument for

the convolver used in [1]–[3], the inequality $x > 16000$, is valid. Equation (18) can be simplified to

$$\sigma^2_{n_r n_r} = c^2_{\mathrm{NL}} \frac{4}{\pi^2} \eta_r^2 \times \left\{ \pi \cdot \omega_g \cdot T_i \left[-\gamma - 4 + \ln\left(\frac{\omega_0}{2\omega_g \sqrt{\omega_0^2 - \omega_g^2}} \right) \right] \right\}. \tag{19}$$

The "worst case" in (18) means that the magnitude of the second part within the outer brackets of (19) is maximized. Neglecting this second part causes an error of around 1%. This gives

$$\sigma^2_{n_r n_r} = c^2_{\mathrm{NL}} \cdot \frac{4}{\pi} \eta_r^2 \omega_g T_i. \tag{20}$$

Since the noise processes $n_r(t)$ and $n_s(t)$ are stationary, we get for the variance of $n_s n_s(t)$

$$\sigma^2_{n_s n_s} = c^2_{\mathrm{NL}} \cdot \frac{4}{\pi} \eta_s^2 \omega_g T_i. \tag{21}$$

The processes $n_r(t)$ and $n_s(t)$ were assumed to be Gaussian distributed and it follows that the processes $n_r n_r(t)$ and $n_s n_s(t)$ are χ^2 distributed with 1° of freedom.

3) Signal Depending Noise Processes: The first process to be considered is $sn_r(t)$. $s(t)$ is given in (4), the noise process $n_r(t)$ is assumed to be stationary, white, Gaussian distibuted, and has a two-sided power spectral density η_r. The power of $sn_r(t)$ is given by

$$P_{sn_r} = \frac{1}{2\pi} \cdot \int_{-\infty}^{\infty} \Phi_{sn_r}(\omega)\, d\omega \tag{22}$$

with $\Phi_{snr}(\omega) = \mathrm{FT}\{\varphi_{snr}(\tau)\}$ and $\varphi_{snr}(\tau) = \mathrm{ACF}\{sn_r(t)\}$. $sn_r(t)$ can be written as

$$\begin{aligned} sn_r(t) &= 2c_{\mathrm{NL}} \cdot \int_{-(T_i/2)}^{T_i/2} s(t+\tau) \cdot n_r(t-\tau)\, d\tau \\ &= \int_{-\infty}^{\infty} s_1(\tau, t) \cdot n_r(2t-\tau)\, d\tau \end{aligned} \tag{23}$$

with $s_1(\tau, t) = 2c_{\mathrm{NL}} \cdot s(\tau) \cdot \mathrm{rect}(2(\tau - t)/T_i)$. Since we are only interested in time intervals where the whole signal $s(t)$ is covered by the integrating electrode and keeping in mind that $n_r(t)$ is stationary, we can simplify the preceding equation to $s_1(\tau) = 2c_{\mathrm{NL}} \cdot s(\tau)$. With that, (23) can be rewritten as

$$sn_r\left(\frac{t}{2}\right) = \int_{-\infty}^{\infty} s_1(\tau) \cdot n_r(t-\tau)\, d\tau = s_1(t) * n_r(t). \tag{24}$$

Similar to $n_r n_r(t)$ [cf (11)], $sn_r(t/2)$ can be considered as the answer of an LTI system with impulse response $s_1(t)$ to the noise process $n_r(t)$ at the input. The relation between the power spectral densities $\Phi_{snr}(\omega)$ and $\Phi_{nr}(\omega)$ of the noise processes $sn_r(t)$ and $n_r(t)$ is given by

$$\Phi_{sn_r}(\omega) = \frac{1}{2} \cdot \Phi_{n_r}\left(\frac{\omega}{2}\right) \cdot \left| S_1\left(j\frac{\omega}{2}\right) \right|^2. \tag{25}$$

With (4), we get for the square of the spectrum of $s_1(2t)$

$$\begin{aligned} &\left| S_1\left(j\frac{\omega}{2}\right) \right|^2 \\ &= 4c^2_{\mathrm{NL}} A_s^2 \\ &\quad \times \left\{ 2\cos(\omega_s T_B + 2\varphi_s) \right. \\ &\qquad \cdot \frac{\sin\left[\left(\frac{\omega}{2} - \omega_s\right)\frac{T_B}{2}\right] \cdot \sin\left[\left(\frac{\omega}{2} + \omega_s\right)\frac{T_B}{2}\right]}{\left(\frac{\omega}{2} - \omega_s\right)\left(\frac{\omega}{2} + \omega_s\right)} \\ &\qquad + \frac{\sin^2\left[\left(\frac{\omega}{2} - \omega_s\right)\frac{T_B}{2}\right]}{\left(\frac{\omega}{2} - \omega_s\right)^2} \\ &\qquad \left. + \frac{\sin^2\left[\left(\frac{\omega}{2} + \omega_s\right)\frac{T_B}{2}\right]}{\left(\frac{\omega}{2} + \omega_s\right)^2} \right\} \cdot n + 8c^2_{\mathrm{NL}} A_s^2 \\ &\quad \times \left\{ 2\cos(\omega_s T_B + 2\varphi_s) \right. \\ &\qquad \cdot \frac{\sin\left[\left(\frac{\omega}{2} - \omega_s\right)\frac{T_B}{2}\right] \cdot \sin\left[\left(\frac{\omega}{2} + \omega_s\right)\frac{T_B}{2}\right]}{\left(\frac{\omega}{2} - \omega_s\right)\left(\frac{\omega}{2} + \omega_s\right)} \\ &\qquad + \frac{\sin^2\left[\left(\frac{\omega}{2} - \omega_s\right)\frac{T_B}{2}\right]}{\left(\frac{\omega}{2} - \omega_s\right)^2} \\ &\qquad \left. + \frac{\sin^2\left[\left(\frac{\omega}{2} + \omega_s\right)\frac{T_B}{2}\right]}{\left(\frac{\omega}{2} + \omega_s\right)^2} \right\} \\ &\quad \times \sum_{k=1}^{n-1} (n-k) \cdot \cos\left(k\frac{\omega}{2} T_C\right). \end{aligned} \tag{26}$$

A numerical investigation of (26) using simulations shows that the part $8c^2_{\mathrm{NL}} A_s^2 \cdot \{\ldots\} \cdot \Sigma(n-k)\cos(k\omega T_c/2)$ can be

neglected. Knowing this, the calculation of the power of $sn_r(t)$ gives the following with (22), (25), and (13):

$$
\begin{aligned}
P_{sn_r} = {} & \frac{4}{\pi}\cdot c_{\mathrm{NL}}^2\eta_r A_s^2 n \\
& \times\left\{\int_{-2(\omega_0+\omega_g)}^{-2(\omega_0-\omega_g)}\cdot\frac{\sin^2\left[(\omega-2\omega_s)\frac{T_B}{4}\right]}{(\omega-2\omega_s)^2}d\omega\right. \\
& \left.+\int_{2(\omega_0-\omega_g)}^{2(\omega_0+\omega_g)}\frac{\sin^2\left[(\omega-2\omega_s)\frac{T_B}{4}\right]}{(\omega-2\omega_s)^2}d\omega\right\} \\
& +\frac{4}{\pi}\cdot c_{\mathrm{NL}}^2\eta_r A_s^2 n \\
& \times\left\{\int_{-2(\omega_0+\omega_g)}^{-2(\omega_0-\omega_g)}\cdot\frac{\sin^2\left[(\omega+2\omega_s)\frac{T_B}{4}\right]}{(\omega+2\omega_s)^2}d\omega\right. \\
& \left.+\int_{2(\omega_0-\omega_g)}^{2(\omega_0+\omega_g)}\frac{\sin^2\left[(\omega+2\omega_s)\frac{T_B}{4}\right]}{(\omega+2\omega_s)^2}d\omega\right\} \\
& +\frac{8}{\pi}\cdot c_{\mathrm{NL}}^2\eta_r A_s^2 n\cdot\cos(\omega_s T_B+2\varphi_s)\times\int_{-2(\omega_0+\omega_g)}^{-2(\omega_0-\omega_g)} \\
& \cdot\frac{\sin\left[(\omega-2\omega_s)\frac{T_B}{4}\right]\cdot\sin\left[(\omega+2\omega_s)\frac{T_B}{4}\right]}{(\omega-2\omega_s)(\omega+2\omega_s)}d\omega \\
& +\frac{8}{\pi}\cdot c_{\mathrm{NL}}^2\eta_r A_s^2 n\cdot\cos(\omega_s T_B+2\varphi_s)\times\int_{2(\omega_0-\omega_g)}^{2(\omega_0+\omega_g)} \\
& \cdot\frac{\sin\left[(\omega-2\omega_s)\frac{T_B}{4}\right]\cdot\sin\left[(\omega+2\omega_s)\frac{T_B}{4}\right]}{(\omega-2\omega_s)(\omega+2\omega_s)}d\omega.
\end{aligned}
\tag{27}
$$

From (27), it is observed that the power P_{snr} has no contribution at $\omega = 0$. Therefore, the relation $P_{snr} = \sigma_{snr}^2$ is valid. Using (17) and $\omega_s = \omega_0$, we can simplify (27) to (28), shown at the bottom of this page.

The approximations as well as the term "worst case" are used in the same sense as was done for (18) and (19). Equation (28) can be simplified to

$$
\begin{aligned}
\sigma_{sn_r}^2 &= \frac{2}{\pi}\cdot c_{\mathrm{NL}}^2\eta_r A_s^2 n\cdot\{T_B + A\} \\
A &= \frac{2}{2\omega_0-\omega_g}+\frac{\cos(\omega_0 T_B+2\varphi_s)}{\omega_0} \\
&\quad\times\left[\pi\cdot\sin(\omega_0 T_B)+\cos(\omega_0 T_B)\cdot\ln\left(\frac{2\omega_0-\omega_g}{2\omega_0+\omega_g}\right)\right].
\end{aligned}
\tag{29}
$$

For real-world convolvers and signals [1]–[3], it can be safely assumed that $T_B \gg A$ holds, and we arrive at the variance of $sn_r(t)$

$$
\sigma_{sn_r}^2 = c_{\mathrm{NL}}^2\cdot 2A_s^2\cdot\eta_r\cdot nT_B. \tag{30}
$$

From (3), it is concluded that the variances of the stationary noise processes $rn_s(t)$, $rn_r(t)$, and $sn_s(t)$ obey similar equations.

$$
\begin{aligned}
\sigma_{sn_r}^2 = {} & \frac{2}{\pi}\cdot c_{\mathrm{NL}}^2\eta_r A_s^2 n\times\left\{\frac{2\omega_g}{4\omega_0^2-\omega_g^2}-\frac{2}{\omega_g}+\underbrace{\frac{\cos[(2\omega_0+\omega_g)T_B]}{2\omega_0+\omega_g}}_{(2\omega_0+\omega_g)^{-1}\text{ (worst case)}}-\underbrace{\frac{\cos[(2\omega_0-\omega_g)T_B]}{2\omega_0-\omega_g}}_{-(2\omega_0-\omega_g)^{-1}\text{ (worst case)}}\right. \\
& \left.+\underbrace{\frac{2\cos(\omega_g T_B)}{\omega_g}}_{2\cdot\omega_g^{-1}\text{ (worst case)}}+\underbrace{T_B\cdot\mathrm{Si}[(2\omega_0+\omega_g)T_B]-T_B\cdot\mathrm{Si}[(2\omega_0-\omega_g)T_B]+2T_B\cdot\mathrm{Si}(\omega_g T_B)}_{\approx\pi\cdot T_B}\right\} \\
& +\frac{2}{\pi}\cdot\frac{c_{\mathrm{NL}}^2\eta_r A_s^2 n}{\omega_0}\cdot\cos(\omega_0 T_B+2\varphi_s)\cdot\cos(\omega_0 T_B) \\
& \times\left\{\ln(2\omega_0-\omega_g)-\ln(2\omega_0+\omega_g)+\underbrace{\mathrm{Ci}[(2\omega_0+\omega_g)T_B]-\mathrm{Ci}[(2\omega_0-\omega_g)T_B]}_{\approx 0}\right\} \\
& +\frac{2}{\pi}\cdot\frac{c_{\mathrm{NL}}^2\eta_r A_s^2 n}{\omega_0}\cdot\cos(\omega_0 T_B+2\varphi_s)\cdot\sin(\omega_0 T_B)\times\left\{\underbrace{2\cdot\mathrm{Si}(\omega_g T_B)}_{\approx\pi}+\underbrace{\mathrm{Si}[(2\omega_0+\omega_g)T_B]-\mathrm{Si}[(2\omega_0-\omega_g)T_B]}_{\approx 0}\right\}.
\end{aligned}
\tag{28}
$$

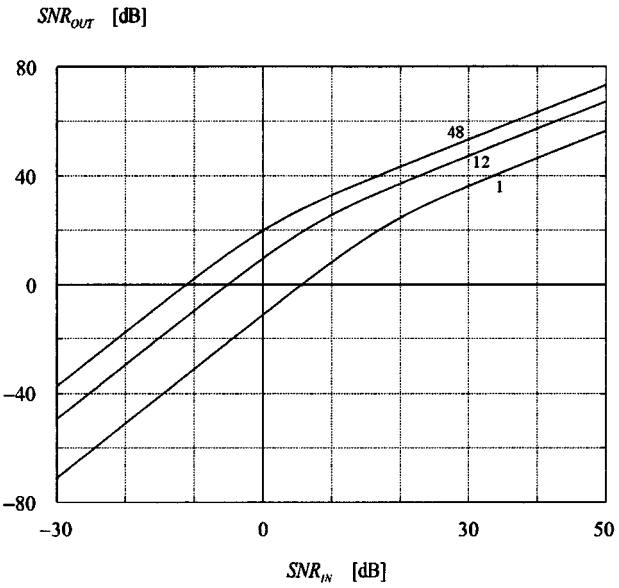

Fig. 4. $\mathrm{SNR_{OUT}}$ at the convolver output depending on $\mathrm{SNR_{IN}}$ at the convolver input for three different code lengths n (1, 12, and 48).

4) SNR at the Convolver Output: The SNR at the convolver output is given by

$$\mathrm{SNR_{OUT}} = \frac{P_{SR}}{\sigma^2_{sn_r}+\sigma^2_{rn_s}+\sigma^2_{rn_r}+\sigma^2_{sn_s}+\sigma^2_{n_rn_r}+\sigma^2_{n_sn_s}} = \frac{(A_sA_rnT_B)^2}{8f_gT_i\cdot(\eta_s^2+\eta_r^2)+2nT_B\cdot(A_s^2+A_r^2)\cdot(\eta_s+\eta_r)}. \tag{31}$$

Using $\mathrm{SNR}_s = A_s^2/(8f_g\eta_s)$ and $\mathrm{SNR}_r = A_r^2/(8f_g\eta_r)$, we can rewrite (31) to

$$\mathrm{SNR_{OUT}} = \frac{8f_gA_s^2A_r^2(nT_B)^2}{X_1+X_2+X_3}$$
$$X_1 = \frac{A_s^4}{\mathrm{SNR}_s}\left(\frac{T_i}{\mathrm{SNR}_s}+2nT_B\right)$$
$$X_2 = \frac{A_r^4}{\mathrm{SNR}_r}\left(\frac{T_i}{\mathrm{SNR}_r}+2nT_B\right)$$
$$X_3 = 2nT_BA_s^2A_r^2\left(\frac{1}{\mathrm{SNR}_s}+\frac{1}{\mathrm{SNR}_r}\right). \tag{32}$$

Since the reference signal is generated in the receiver, the unequation $\mathrm{SNR}_r \gg \mathrm{SNR}_s\ (=\mathrm{SNR_{IN}})$ holds. Considering this and adjusting the amplifiers at the convolver inputs in a way that $A_s = A_r$, we obtain

$$\mathrm{SNR_{OUT}} = \frac{2f_g\cdot(nT_B)^2\cdot\mathrm{SNR_{IN}}}{nT_B+\dfrac{T_i}{4\cdot\mathrm{SNR_{IN}}}} \quad \text{or}$$

$$\mathrm{SNR_{OUT}^{[dB]}} = \mathrm{SNR_{IN}^{[dB]}} + 10\cdot\log\left[\frac{2f_g\cdot nT_B}{1+\dfrac{T_i/T_B}{4n\cdot\mathrm{SNR_{IN}^{[lin.]}}}}\right]. \tag{33}$$

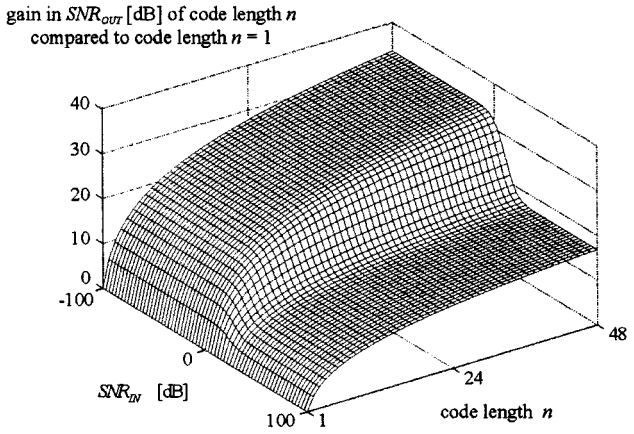

Fig. 5. Gain in $\mathrm{SNR_{OUT}}$ at the convolver output depending on the $\mathrm{SNR_{IN}}$ at the convolver input and code length n compared to code length $n = 1$.

From [1]–[3], we have data of a convolver and used signals, $T_i = 16\ \mu$s, $f_g = 80$ MHz, and $T_B = 70$ ns. Fig. 4 shows the $\mathrm{SNR_{OUT}}$ at the convolver output dependent on the $\mathrm{SNR_{IN}}$ at the convolver input for three different code lengths. One can see that the χ^2 distributed part is dominating for $\mathrm{SNR_{IN}} < 0,\ldots,10$ dB, whereas the Gauss distributed part is dominating for $\mathrm{SNR_{IN}} > 10,\ldots,20$ dB. In the literature (e.g., [8]), the χ^2 distributed part is neglected. As we see from Fig. 4, this is only permissible for an $\mathrm{SNR_{IN}} > 10,\ldots,20$ dB; values that are often not reached in spread-spectrum communications. Fig. 5 depicts the gain of $\mathrm{SNR_{OUT}}$ that can be achieved with code lengths n compared to a code length $n = 1$. The transition from the χ^2 distribution dominated part to the Gauss distribution dominated part can be recognized very well.

IV. Conclusions

The noise behavior at the output of a SAW convolver is derived and discussed for matched filter applications. In view of these applications, one input signal is assumed to be generated locally in the receiver as the reference signal. Therefore, its SNR is much higher than the received signal at the second input of the convolver. We calculated the instantaneous SNR at the convolver output at the sampling time, which is dependent on the SNR at the receiving signal input of the convolver. It was shown that the noise processes with squared amplitudes contribute significantly to the noise at the output for $\mathrm{SNR_{IN}} < 10$ dB. Neglecting these quadratic contributions causes a significant error (up to some 10 dB) in the $\mathrm{SNR_{OUT}}$.

Acknowledgment

The author thanks Dr. F. Seifert (retired), Applied Electronics Laboratory, University of Technology, Vienna, Austria, and Dr. A. Pohl, Siemens AG, Vienna, Austria, for continuous scientific advice and stimulating discussions. The authors also gratefully acknowledge Dr. L. Reindl, Institute of Electrical Information Technology, Technical University Clausthal, Clausthal, Germany, for helpful discussions.

REFERENCES

[1] W. Pietsch and F. Seifert, "Measurements of radio channels using an elastic convolver and spread spectrum modulation: Part I—Implementation," *IEEE Trans. Instrum. Meas.*, vol. 43, pp. 689–694, Oct. 1994.

[2] W. Pietsch, "Measurements of radio channels using an elastic convolver and spread spectrum modulation: Part II—Results," *IEEE Trans. Instrum. Meas.*, vol. 43, pp. 695–699, Oct. 1994.

[3] G. Ostermayer, A. Pohl, C. Hausleitner, L. Reindl, and F. Seifert, "CDMA for wireless SAW sensor applications," in *Proc. IEEE Int. Spread-Spectrum Tech. Applicat. Symp.*, 1996, pp. 795–799.

[4] A. Pohl, C. Posch, L. Reindl, and F. Seifert, "Digitally controlled compressive receiver," in *Proc. IEEE Int. Spread-Spectrum Tech. Applicat. Symp.*, 1996, pp. 409–413.

[5] G. Schrom, "Messung der wignerverteilung mit SAW—Convolver," Masters thesis, Appl. Electron. Lab., Univ. Technol., Vienna, Austria, Feb. 1992.

[6] H.-P. Graßl, "Entwurf und analyse von akustischen oberflächenwellen—Convolver," Ph.D. dissertation, Appl. Electron. Lab., Univ. Technol., Vienna, Austria, 1984.

[7] R. M. White and F. W. Voltmer, "Direct piezoelectric coupling to surface elastic waves," *Appl. Phys. Lett.*, vol. 7, pp. 314–316, 1965.

[8] A. Chatterjee, P. Das, and L. Milstein, "The use of SAW convolvers in spread-spectrum and other signal-processing applications," *IEEE Trans. Sonics Ultrason.*, vol. SU-32, pp. 745–759, Sept. 1985.

[9] H. Weinrichter and F. Hlawatsch, *Stochastische Grundlagen Nachrichtentechnischer Signale*. Berlin, Germany: Springer-Verlag, 1991, p. 107.

[10] W. Davenport and W. Root, *An Introduction to the Theory of Random Signals and Noise*. New York: IEEE Press, 1987, p. 255.

[11] M. Abramowitz and I. Stegun, *Handbook of Mathematical Functions* New York, 1970, pp. 231–238.

Gerald Ostermayer (S'98–A'99) received the Dipl.-Ing. and Dr.techn. degrees in communication engineering from the University of Technology (TU), Vienna, Austria, in 1992 and 1998, respectively. His doctoral research described the use of correlative signal processing in SAW sensor systems.

In 1992, he joined EBG, where he was a Design Engineer involved with high-voltage power transformers. In 1994, he joined the Applied Electronics Laboratory, Institut für Allgemeine Elektrotechnik und Elektronik, TU, where he was a Research and Teaching Assistant. In 1997, he joined PSE MCS RA2, Siemens AG Österreich, Vienna, Austria, during which time he has been involved in the field of third-generation (3G) mobile systems. His research interests are in the areas of network simulation and radio resource management (RRM) algorithms for 3G mobile systems.